Optimal Reactive Power Dispatch for Voltage Regulation in Unbalanced Distribution Systems

Brett A. Robbins, *Student Member, IEEE* and Alejandro D. Domínguez-García, *Member, IEEE*

***Abstract*—In this paper, we propose a method to optimally set the reactive power contributions of distributed energy resources (DERs) present in distribution systems with the goal of regulating bus voltages. For the case when the network is balanced, we use the branch power flow modeling approach for radial power systems to formulate an optimal power flow (OPF) problem. Then, we leverage properties of the system operating conditions to relax certain nonlinear terms of this OPF, which results in a convex quadratic program (QP). To efficiently solve this QP, we propose a distributed algorithm based on the Alternating Direction Method of Multipliers (ADMM). Furthermore, we include the unbalanced three-phase formulation to extend the ideas introduced for the balanced network case. We present several case studies to demonstrate the method in unbalanced three-phase distribution systems.**

***Index Terms*—Distributed Algorithms, Relaxation Methods, Decentralized Control, Power System Analysis Computing, Reactive Power Control, ADMM.**

I. Introduction

THE introduction of distributed energy resources (DERs), e.g., plug-in hybrid electric vehicles (PHEV) and photovoltaic installations (PV), in distribution systems results in operational scenarios that these systems were not designed to handle. Interestingly, by properly controlling the power electronic grid interfaces of these DERs, they can provide reactive power support for voltage regulation; thus, helping to mitigate the variability introduced by uncontrolled active power injections of certain types of DERs, e.g., PV installations [1]. The current control of DERs is limited in the sense that these devices generally do not provide reactive power for voltage regulation and they operate with local policies designed to protect the grid during severe operating conditions [2]. This paper proposes a method to optimally set the reactive power contributions of the DERs to regulate distribution system voltages to a desired reference value.

In order to address the voltage control problem in distribution systems, we envision a two time-scale architecture that classifies voltage control devices as either slow or fast time-scale actuators, with the idea of controlling them separately. Conventional voltage regulation devices, e.g., TCUL transformers and switched capacitors, which would be considered slow time-scale actuators, are dispatched in time-scales ranging from minutes to hours; whereas power-electronic-interfaced DERs with reactive power provision capability would be the latter and are controlled in time-scales ranging from milliseconds to seconds. Periodically, the slow time-scale control will dispatch the associated actuators, which would result in some voltage profile [3]; this is intended to reduce the mechanical wear on legacy devices so as to prolong their lifetimes [4]. The slow time-scale control can be performed based on heuristics associated with the time of day, or the system can be monitored for contingency cases, e.g., system voltages being outside of tolerances. Then, given that fast (and uncontrolled) changes in DER active generation (consumption) might cause the voltage to deviate from the voltage profile set by the slow time-scale optimization, a second optimization or a feedback control scheme executed at regular intervals could be utilized to determine the active/reactive power settings of the DERs. This paper intends to address this latter problem by providing an optimal scheme to handle voltage regulation during the inter-time periods between slow time-scale dispatches.

First, we formulate this voltage regulation problem for a balanced network as a quadratic program (QP) around the operating point determined by the procedure we proposed in [3], which optimally sets voltage regulation transformers and provides limited reactive power support. To this end, we leverage a variant of the branch flow model formulation known as the DistFlow (see, e.g., [5]–[7]). This will allow us to make similar simplifications to those made by the authors of [4], [8], and formulate a problem that has linear constraints with a quadratic cost function, which is a convex problem around a particular operating point. Then, we extend the aforementioned formulation for balanced systems to the unbalanced three-phase case by using a similar approach to the linear approximation mentioned in [9]. Finally, in order to efficiently solve these QP problems, we propose a distributed algorithm based on the Alternating Direction Method of Multipliers (ADMM) [10]. Consequently, we can retain the communication network and partitions established by the distributed solver for the slow time-scale optimization proposed in [3].

The DistFlow is a well-established method that recursively solves the power flow for strictly radial systems; it was originally proposed in [5]–[7]. The authors in [11] extended this concept to include branches for both tree networks and mesh networks. This power flow formulation has a distinct advantage in that the bus phase angles are irrelevant for a balanced network (described by its per-phase equivalent) since they are expressed as line power flows and voltage magnitudes.

B. A. Robbins and A. D. Domínguez-García are with the Department of Electrical and Computer Engineering, University of Illinois at Urbana-Champaign, Urbana, IL, 61801. E-mail: {robbins3, aledan}@ILLINOIS.EDU.

This research was supported in part by the National Science Foundation (NSF) under CAREER Award ECCS-CAR-0954420, and by ABB under project "Distributed and Resilient Voltage Control of Distributed Energy Resources in the Smart Grid" (University of Illinois contract UIeRA 2013-2955-00-00).

Unfortunately, the power flow and voltage constraints have a nonlinear power loss term that makes the problem non-convex. The authors in [11], [12] provide a lower bound on the losses with a second-order cone program (SOCP). In this case, the solution to the SOCP relaxation is exact when equality on the lower bound is satisfied. Recently, the authors of [4], [8] used the DistFlow to formulate, by neglecting the nonlinear terms, a convex quadratic optimal power flow (OPF) to determine the reactive power support provided by inverters in systems with high penetration of PV installations. Our approach in this paper approximates the nonlinear terms as constants that are periodically updated based on the desired operating point since we found that the loss terms, in general, cannot be entirely neglected. Unlike the SOCP-based OPF, the intended purpose of the fast time-scale control is to maintain the globally optimal solution from the slow time-scale optimization, rather than finding a global minimum for the entire solution space.

The control and optimization of DERs is generally broken down into three different categories: (i) centralized, (ii) distributed, and (iii) local (decentralized) schemes. Centralized-based methods include branch flow formulations [4], [8], [11], second-order cone program (SOCP) [9], [11], and rank-relaxed semidefinite program (SDP) formulations (see e.g., [3], [13]–[15] and the references therein). Lately, rank-relaxed SDP-based formulations have gathered significant attention. While this approach is not guaranteed to provide a global minimum, e.g., it can fail for tightly constrained mesh networks, it has been shown that the solution to the SDP-based OPF will return a rank-1 solution for tree-structure networks under some mild conditions [14], [16], [17]; these structures are typical of radial distribution systems. In this case, the SDP-approach guarantees a global minimum. Then, the convex optimization can be solved distributively with either a subgradient- or an ADMM-based distributed algorithm [3], [12], [14], [15]. Otherwise, DERs can be controlled through a local scheme that consists of a local feedback controller [18], [19], or policies that are designed to maintain grid reliability [2]. Our proposed QP-based formulation can be solved by either a centralized or a distributed solver. In this paper, we use ADMM to solve the QP-based OPF problem in a distributed fashion due to its previous success in power system applications [3], [20], [21]. In this regard, the ability to perform the optimization tasks in parallel can dramatically reduce computation time and complexity for large-scale systems [21].

The SDP-based and SOCP-based optimizations are designed to capture the nonconvexities of the network with the goal of finding a globally optimal solution for the system-wide set of optimization variables and constraints. In contrast, the approach for voltage regulation proposed in this paper minimizes the voltage deviations from the reference voltage determined by the latest dispatch of the slow time-scale optimization proposed in [3]. This implies that the behavior of the system is nearly linear around the desired operating point. The primary advantage of the QP-based OPF over the SDP-based OPF is that the complexity of the problem scales linearly, rather than exponentially with the number of system buses, and the QP can be solved fast enough with sufficient accuracy. Similar to the SOCP-based method proposed in [11], the proposed QP-based OPF proposed in this paper leverages an angle relaxation to formulate the optimization problem in terms of voltage magnitude and distribution line segment power flows without a dependence on the bus angles. The angle relaxation is exact for balanced radial and mesh networks, but the SOCP is not suited for the unbalanced three-phase case. This is due to the fact that the mutual impedance of the distribution line segments in the unbalanced three-phase system introduces a coupling between the phases that complicates both the angle and conic relaxations of the SOCP. While a similar linearization to the one we propose can be applied to the SOCP, the validity of the lower bound on the nonlinear system losses is uncertain.

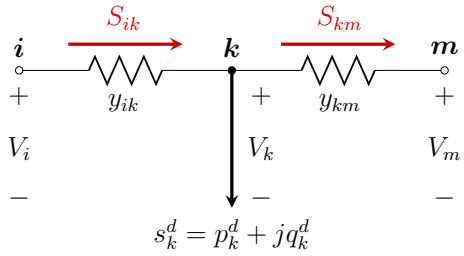

Figure 1: Distribution line segment power flows.

The remainder of this paper is organized as follows. Section II introduces the system model that we adopt in this work and formulates the voltage regulation problem. In Section III, we rewrite the OPF as a convex QP and extend the per-phase equivalent formulation to the unbalanced three-phase case. The proposed ADMM-based distributed solver is formulated in Section IV. Section V presents the case studies and concluding remarks are presented in Section VI.

II. Problem Formulation

In this section, we introduce the power flow formulation adopted in this work. Then, in order to solve the voltage regulation problem, we formulate an optimal power flow.

A. Branch Power Flow Formulation

Consider an $n+1$ bus power distribution system with a tree topology, i.e., a radial network without loops between the branches. We index the feeder by 0, and let the elements in the set $\mathcal{N} := \{1, 2, \ldots, n\}$ index the remaining n buses of the system. The edge-set that represents the set of distribution line segments (which could contain conductors for single-, two-, or three-phase circuits) is denoted by $\mathcal{E} \subseteq \{\mathcal{N} \cup \{0\}\} \times \{\mathcal{N} \cup \{0\}\}$, with $(i,k) \in \mathcal{E}$ if there is a distribution line segment between buses i and k, where bus i is closest to the feeder, i.e., in our notation the edges are directed so that $(i,k) \in \mathcal{E} \Rightarrow (k,i) \notin \mathcal{E}$. The impedance for the distribution line segment (i,k) is given by $z_{ik} = r_{ik} + jx_{ik}$. We ignore line charging (shunt capacitance) since lines in distribution systems are typically so short that this admittance can be neglected [22]. The demand at bus k is denoted by $s_k^d = p_k^d + jq_k^d$.

Consider the circuit shown in Fig. 1; we will formulate the voltage drop and power flow equations between buses i and

k using the notation and orientation shown in the figure. Let $\mathcal{H}_k := \{j \,|\, (k,j) \in \mathcal{E}\}$ be the set of buses downstream of bus k; then, the total power $S_{ik} \in \mathbb{C}$ transferred through the distribution line segment (i,k) is

$$S_{ik} = \sum_{j \in \mathcal{H}_k} S_{kj} + s_k^d + z_{ik} \frac{|S_{ik}|^2}{|V_i|^2}, \tag{1}$$

where the line power flow S_{ik} is always determined relative to the sending end voltage, $V_i = |V_i| \angle \theta_i$, of the distribution line segment. We compute the voltage of bus k based on the upstream bus i with

$$V_k = V_i - z_{ik} \frac{P_{ik} - jQ_{ik}}{V_i^*}, \tag{2}$$

where the feeder's voltage is fixed, i.e., $V_0 = V^s = |V^s| \angle 0$, for some constant $|V^s|$. We can remove the dependence on the phase angles in (2) by taking the product of each side of (2) with its conjugate. Thus, the branch model of the power flow equations for an $n+1$ bus network are given by

$$V_0 = V^s, \tag{3a}$$

$$|V_k|^2 = |V_i|^2 - 2\left(r_{ik}P_{ik} + x_{ik}Q_{ik}\right) + |z_{ik}|^2 \frac{|S_{ik}|^2}{|V_i|^2}, \tag{3b}$$

$$P_{ik} = \sum_{j \in \mathcal{H}_k} P_{kj} + p_k^d + r_{ik} \frac{|S_{ik}|^2}{|V_i|^2}, \tag{3c}$$

$$Q_{ik} = \sum_{j \in \mathcal{H}_k} Q_{kj} + q_k^d + x_{ik} \frac{|S_{ik}|^2}{|V_i|^2}, \tag{3d}$$

for all $(i,k) \in \mathcal{E}$. This is a natural extension of the DistFlow model originally proposed in [5], [6], which formulates the line power transfer (3c)–(3d) so that the power flow can be solved recursively for a strictly radial system. The updated expressions in (3c)–(3d) are designed to handle branches in a tree network and are similar to the branch flow approach proposed in [11] to accommodate both radial and mesh networks.

B. Voltage Regulation Problem

In our previous work in [3], we performed a slow timescale optimization to fix transformer tap positions so as to establish a voltage magnitude reference, $V^r \in \mathbb{R}^n$, that meets certain operational specifications for the system, i.e., minimize system losses, flatten the voltage profile, or achieve some power factor correction target. Then, bus voltages can be regulated to V^r during the inter-dispatch time periods by controlling the reactive power contributions of the aggregated DERs connected to the system buses. Ideally, we would like to determine the amount of reactive power support needed to track V^r as the load fluctuates; however, there may not exist a feasible solution given the current operating conditions and the lower and upper reactive power limits on the reactive power capable DERs, $\underline{q}, \overline{q}$, respectively. Thus, we perform an optimization to minimize the voltage deviations from V^r.

Let $\mathcal{N} = \mathcal{N}_c \cup \mathcal{N}_u$, $\mathcal{N}_c \cap \mathcal{N}_u = \emptyset$, where $\mathcal{N}_c$ and $\mathcal{N}_u$ are the sets of buses that have controllable and uncontrolled (or without) reactive power resources, respectively. We define q_k to be the total reactive power contributions of the DERs connected to the buses in $\mathcal{N}_c$. Then, we can perform the following optimization

$$\min_{V} \sum_{k=1}^{n} w_k \left(|V_k|^2 - (V_k^r)^2 \right)^2 \tag{4a}$$

such that, for all $(i,k) \in \mathcal{E}$,

$$V_0 = V^s, \tag{4b}$$

$$|V_k|^2 = |V_i|^2 - 2(r_{ik}P_{ik} + x_{ik}Q_{ik}) + |z_{ik}|^2 \frac{|S_{ik}|^2}{|V_i|^2}, \ k \in \mathcal{N}, \tag{4c}$$

$$P_{ik} = \sum_{j \in \mathcal{H}_k} P_{kj} + p_k^d + r_{ik} \frac{|S_{ik}|^2}{|V_i|^2}, \qquad k \in \mathcal{N}, \tag{4d}$$

$$Q_{ik} = \sum_{j \in \mathcal{H}_k} Q_{kj} + q_k^d + x_{ik} \frac{|S_{ik}|^2}{|V_i|^2} - q_k, \qquad k \in \mathcal{N}_c, \tag{4e}$$

$$Q_{ik} = \sum_{j \in \mathcal{H}_k} Q_{kj} + q_k^d + x_{ik} \frac{|S_{ik}|^2}{|V_i|^2}, \qquad k \in \mathcal{N}_u, \tag{4f}$$

and

$$\underline{q}_k \le q_k \le \overline{q}_k, \qquad k \in \mathcal{N}_c. \tag{4g}$$

The weighting term $w_k > 0$ in (4a) can be chosen based on heuristics, e.g., larger penalties will be given to buses that are most susceptible to voltage violations. We can incorporate the fixed transformer tap positions by replacing $|V_i|^2$ in (4c)–(4f) with $|V_i|^2 / a_{ik}^2$, where a_{ik} is the per-unit turns ratio of the voltage regulator connected to the upstream bus i. The benefit of the branch flow approach is that we are able to remove all dependencies on the phase angles; however, the problem is still nontrivial due to the nonlinear terms in the equality constraints. Hence, in the ensuing section we will discuss how to relax the OPF in (4).

III. Convex Relaxation

In this section, we make the necessary relaxations to reformulate the OPF problem in (4) as a convex quadratic program (QP) with linear constraints. Then, we develop the equivalent formulation for the three-phase unbalanced case.

A. Linearization of the Power Flow Equations

We found experimentally for the systems in Section V, that for mild loading conditions, the nonlinear loss terms in (4c)–(4f) behaved linearly, and in some instances, they can be ignored entirely. For example, the nonlinear term in the voltage relationship (4c) was found to be 3-6 orders of magnitude smaller than the other terms and could be considered negligible, which is consistent with the results in [4], [8]. Despite the relative size of these terms, we found that the optimization results were more accurate when we treated them as constants or as linear approximations rather than ignoring them entirely. The nonlinear terms in the active power flow constraints (4d) were found to be 2-3 orders of magnitude smaller than the line flows. In contrast, the reactive power constraints (4e)–(4f) can be very sensitive to the line flows. This is particularly apparent under heavy active power loading and significant reactive power support, e.g., $P_{ik} >> Q_{ik}$ implies $S_{ik} \propto P_{ik}$

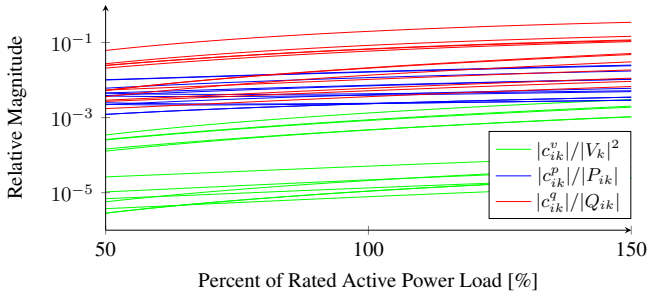

Figure 2: Relative magnitude of the nonlinear terms.

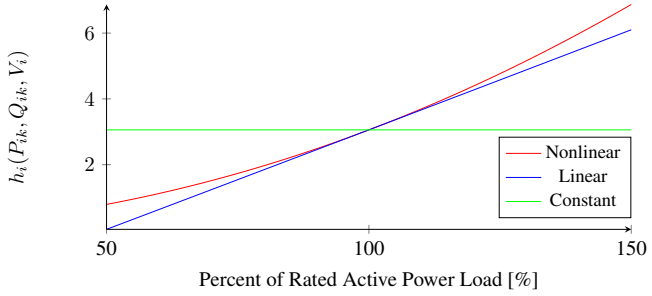

Figure 3: Behavior of the nonlinear terms.

becomes large and the reactive power Q_{ik} diminishes since q_k is perceived as a *negative* load. Figure 2 shows the relative magnitudes of the nonlinear terms according to their respective equality constraint for every bus in the balanced case of the 15-bus network shown in Fig. 4; where we uniformly vary the active power loads and rerun the power flow. Note that we represent the nonlinear terms for the voltage, active power, and reactive power constraints along the distribution line segment (i,k) as $c^v_{ik}(P,Q)$, $c^p_{ik}(P,Q)$, and $c^q_{ik}(P,Q)$, respectively.

The nonlinearity in the constraints (4c)–(4f) for the distribution line segment $(i,k) \in \mathcal{E}$ attached to bus i is given by

$$h_{ik}\left(P,Q\right) = \frac{P_{ik}^2 + Q_{ik}^2}{|V_i|^2}, \tag{5}$$

and we define the functions

$$c^v_{ik}(P,Q) = |z_{ik}|^2 h_{ik}\left(P,Q\right), \tag{6a}$$
$$c^p_{ik}(P,Q) = r_{ik} h_{ik}\left(P,Q\right), \tag{6b}$$
$$c^q_{ik}(P,Q) = x_{ik} h_{ik}\left(P,Q\right), \tag{6c}$$

to represent the nonlinear loss terms for the voltage, active power, and reactive power equality constraints, respectively. Then, we approximate the system model by

(i) treating the $c_{ik}(P,Q)$'s as constants computed from the initial distribution line segment power flows P_{ik_o}, Q_{ik_o} and the reference voltage V_i^r, or

(ii) using a linear approximation of the nonlinear terms based on the current distribution line segment power flows $P_{ik} + jQ_{ik}$ and the reference voltage V_i^r.

We linearize (5) around the operating point (P_o, Q_o, V^r) with the first-order approximation

$$h_{ik}(P,Q) \approx \frac{1}{|V_i^r|^2}\left[2P_{ik_o}P_{ik} + 2Q_{ik_o}Q_{ik} - |S_{ik_o}|^2\right], \tag{7}$$

where the reference voltage V^r is fixed. Figure 3 shows the behavior of the nonlinear loss terms and compares it against the linear and constant approximations for the 15-bus system where we vary the active power on every bus. The linear approximation is clearly a better fit; however, Fig. 3 represents an extreme case where there is a $\pm 50\%$ change in the active load for every bus in the network. For relatively small changes in system loads around the desired operating point, the constant approximation produces acceptable results, which we will show in Section V.

B. Relaxed OPF for Balanced Systems

Applying the linear approximation of the power flow constraints, the OPF problem in (4) simplifies to a QP. The power flow constraints in (4d)–(4f) do not depend on bus voltages, and the square of the voltage magnitudes in (4a)–(4c) can be replaced by the variables $U_i = |V_i|^2$ and $U_i^r = (V_i^r)^2$. Thus, the equivalent problem has a quadratic cost function with linear constraints, and can be formulated as follows:

$$\min_{U} \sum_{k=1}^{n} w_k \left(U_k - U_k^r\right)^2 \tag{8a}$$

such that, for all $(i,k) \in \mathcal{E}$,

$$U_0 = |V^s|^2, \tag{8b}$$
$$U_k = U_i - 2(r_{ik}P_{ik} + x_{ik}Q_{ik}) + c^u_{ik}(P,Q)\,, \quad k \in \mathcal{N}, \tag{8c}$$
$$P_{ik} = \sum_{j \in \mathcal{H}_k} P_{kj} + p_k^d + c^p_{ik}\left(P,Q\right), \quad k \in \mathcal{N}, \tag{8d}$$
$$Q_{ik} = \sum_{j \in \mathcal{H}_k} Q_{kj} + q_k^d + c^q_{ik}\left(P,Q\right) - q_k, \quad k \in \mathcal{N}_c, \tag{8e}$$
$$Q_{ik} = \sum_{j \in \mathcal{H}_k} Q_{kj} + q_k^d + c^q_{ik}\left(P,Q\right), \quad k \in \mathcal{N}_u, \tag{8f}$$

and

$$\underline{q}_k \le q_k \le \overline{q}_k, \qquad k \in \mathcal{N}_c, \tag{8g}$$

where we update the notation of c^v_{ik} to c^u_{ik} accordingly. In Section V, we explore variations of (8) where we recompute the c_{ik}'s based on the dispatch system state or update the line flows P and Q with the current operating conditions.

C. Extension to Unbalanced Three-Phase Systems

Up to this point, we have only considered the case when the phases are balanced; however, distribution systems are inherently unbalanced with untransposed distribution line segments, and have single-, two-, and three-phase radial feeds. Therefore, extending the ideas discussed for far to unbalanced three-phase systems is well motivated [9], [20]. Unfortunately, the coupling between phases for the system voltages in (8c) requires additional approximations to simplify the unbalanced case to a QP problem.

For each $(i,k) \in \mathcal{E}$, let

$$\boldsymbol{V}_k = \boldsymbol{V}_i - \boldsymbol{z}_{ik}\left[(\boldsymbol{P}_{ik} - j\boldsymbol{Q}_{ik}) \oslash \boldsymbol{V}_i^*\right], \tag{9}$$

where $\boldsymbol{V}_i = [V_{i_a}, V_{i_b}, V_{i_c}]^{\mathrm{T}}$, $\boldsymbol{V}_k = [V_{k_a}, V_{k_b}, V_{k_c}]^{\mathrm{T}}$, $\boldsymbol{P}_{ik} = [P_{ik_a}, P_{ik_b}, P_{ik_c}]^{\mathrm{T}}$, $\boldsymbol{Q}_{ik} = [Q_{ik_a}, Q_{ik_b}, Q_{ik_c}]^{\mathrm{T}}$, and $\boldsymbol{z}_{ik} \in \mathbb{C}^{3\times 3}$, and $\oslash$ and $\odot$ denote the element-wise division and

multiplication, respectively. [This is essentially an extension of (2) to the three-phase case.]

Unlike the per-phase equivalent case, multiplying by the complex conjugate of both side of (9) will not remove the dependence on $\boldsymbol{\theta}$. This is due to the fact that there is a coupling between the phases at bus i that arises from the cross-products of the three-phase equations for the phase voltages and line currents. To address this, we have observed that the voltage magnitudes between the phases are similar, i.e., $|V_{i_a}| \approx |V_{i_b}| \approx |V_{i_c}|$, and that the phase unbalances on each bus are not very severe, so we assume that the voltages are nearly balanced. This enables us to approximate the phase differences at bus i as

$$\begin{aligned}\cos\left(\theta_{i_a}-\theta_{i_b}\right) &= \cos\left(\frac{2\pi}{3}+\alpha\right)\\ &= -\frac{1}{2}\cos\left(\alpha\right)-\frac{\sqrt{3}}{2}\sin\left(\alpha\right)\approx -\frac{1}{2},\end{aligned} \tag{10}$$

and similarly

$$\sin\left(\theta_{i_a}-\theta_{i_b}\right)=\sin\left(\frac{2\pi}{3}+\alpha\right)\approx\frac{\sqrt{3}}{2}, \tag{11}$$

where α represents the relative phase unbalance, which is sufficiently small [9]. We can update the voltage magnitude constraint in (8c) for the unbalanced case with

$$|\boldsymbol{V}_k|^2 = |\boldsymbol{V}_i|^2 - 2\left(\tilde{\boldsymbol{r}}_{ik}\boldsymbol{P}_{ik}+\tilde{\boldsymbol{x}}_{ik}\boldsymbol{Q}_{ik}\right)+\boldsymbol{c}^u_{ik}(\boldsymbol{P},\boldsymbol{Q}), \tag{12}$$

where

$$\boldsymbol{a}=\begin{bmatrix}1 & e^{-j2\pi/3} & e^{j2\pi/3}\end{bmatrix}^{\mathrm{T}}, \tag{13}$$

$$\tilde{\boldsymbol{r}}_{ik}=\mathrm{Re}\left\{\boldsymbol{a}\boldsymbol{a}^{\mathrm{H}}\right\}\odot\boldsymbol{r}_{ik}+\mathrm{Im}\left\{\boldsymbol{a}\boldsymbol{a}^{\mathrm{H}}\right\}\odot\boldsymbol{x}_{ik}, \tag{14}$$

$$\tilde{\boldsymbol{x}}_{ik}=\mathrm{Re}\left\{\boldsymbol{a}\boldsymbol{a}^{\mathrm{H}}\right\}\odot\boldsymbol{x}_{ik}-\mathrm{Im}\left\{\boldsymbol{a}\boldsymbol{a}^{\mathrm{H}}\right\}\odot\boldsymbol{r}_{ik}, \tag{15}$$

for all $(i,k)\in\mathcal{E}$. We refer the reader to Appendix A for the unbalanced phase approximations of (12)–(15). The linear approximations of $\boldsymbol{c}^u_{ik}(\boldsymbol{P},\boldsymbol{Q})$, $\boldsymbol{c}^p_{ik}(\boldsymbol{P},\boldsymbol{Q})$, and $\boldsymbol{c}^q_{ik}(\boldsymbol{P},\boldsymbol{Q})$ for the unbalanced three-phase case are provided in Appendix B; however, for the case where we represent the terms as constants, we have

$$\boldsymbol{c}^u_{ik}(\boldsymbol{P},\boldsymbol{Q})=\left[\boldsymbol{z}_{ik}\left[\boldsymbol{S}^*_{ik_o}\oslash(\boldsymbol{V}^{r_o}_i)^*\right]\right]\odot\left[\boldsymbol{z}^*_{ik}\left[\boldsymbol{S}_{ik_o}\oslash\boldsymbol{V}^{r_o}_i\right]\right], \tag{16}$$

$$\boldsymbol{c}^p_{ik}(\boldsymbol{P},\boldsymbol{Q})=\mathrm{Re}\left\{\left[\boldsymbol{S}_{ik_o}\oslash\boldsymbol{V}^{r_o}_i\right]\odot\left(\boldsymbol{V}^{r_o}_i-\boldsymbol{V}^{r_o}_k\right)\right\}, \tag{17}$$

$$\boldsymbol{c}^q_{ik}(\boldsymbol{P},\boldsymbol{Q})=\mathrm{Im}\left\{\left[\boldsymbol{S}_{ik_o}\oslash\boldsymbol{V}^{r_o}_i\right]\odot\left(\boldsymbol{V}^{r_o}_i-\boldsymbol{V}^{r_o}_k\right)\right\}, \tag{18}$$

where $\boldsymbol{V}^{r_o}\in\mathbb{C}^3$ is the complex voltage for the initial dispatch of the reference voltage $\boldsymbol{V}^r\in\mathbb{R}^3$.

We express the unbalanced three-phase voltage regulation QP-based OPF as

$$\min_{\boldsymbol{U}}\sum_{k=1}^{n}\left\|\boldsymbol{w}_k\odot\left(\boldsymbol{U}_k-\boldsymbol{U}^r_k\right)\right\|_2^2 \tag{19a}$$

such that, for all $(i,k)\in\mathcal{E}$,

$$\boldsymbol{U}_0=|\boldsymbol{V}^s|\odot|\boldsymbol{V}^s|, \tag{19b}$$

$$\boldsymbol{U}_k=\boldsymbol{U}_i-2\left(\tilde{\boldsymbol{r}}_{ik}\boldsymbol{P}_{ik}+\tilde{\boldsymbol{x}}_{ik}\boldsymbol{Q}_{ik}\right)+\boldsymbol{c}^u_{ik}(\boldsymbol{P},\boldsymbol{Q}),\ k\in\mathcal{N}, \tag{19c}$$

$$\boldsymbol{P}_{ik}=\sum_{j\in\mathcal{H}_k}\boldsymbol{P}_{kj}+\boldsymbol{p}^d_k+\boldsymbol{c}^p_{ik}(\boldsymbol{P},\boldsymbol{Q}),\qquad k\in\mathcal{N}, \tag{19d}$$

$$\boldsymbol{Q}_{ik}=\sum_{j\in\mathcal{H}_k}\boldsymbol{Q}_{kj}+\boldsymbol{q}^d_k+\boldsymbol{c}^q_{ik}(\boldsymbol{P},\boldsymbol{Q})-\boldsymbol{q}_k,\qquad k\in\mathcal{N}_c, \tag{19e}$$

$$\boldsymbol{Q}_{ik}=\sum_{j\in\mathcal{H}_k}\boldsymbol{Q}_{kj}+\boldsymbol{q}^d_k+\boldsymbol{c}^q_{ik}(\boldsymbol{P},\boldsymbol{Q}),\qquad k\in\mathcal{N}_u, \tag{19f}$$

and

$$\underline{\boldsymbol{q}}_k\le\boldsymbol{q}_k\le\overline{\boldsymbol{q}}_k,\qquad k\in\mathcal{N}_c. \tag{19g}$$

Note that this will reduce to (8) for a balanced system.

IV. Distributed Algorithm

As we mentioned earlier, there are several advantages that motivate the use of a distributed solver to solve the QP-based OPF in Section III; in this section, we propose the use of ADMM to develop such a solver. ADMM has been proven to be a powerful solution to develop distributed algorithms [10]; in particular, with ADMM, the complexity of the OPF problem scales with the sub-area size rather than with the full network size, and the communication architecture is simpler than that of a centralized scheme. ADMM iteratively minimizes the augmented Lagrangian over three types of variables: (i) the *primary* variables, i.e., the bus voltages and line power flows; (ii) the *auxiliary* variables that are used to enforce boundary conditions among neighboring areas; and (iii) the *multipliers* for dualizing the relaxed problem. The Lagrangian is designed to be separable relative to each type of variable so that we can cyclically minimize with respect to one variable type while fixing the others. This allows us to solve the problem distributively and asymptotically converge to the same minimum costs obtained with a centralized solver [10].

For each node, let $\mathcal{B}_k$ denote the set that captures the voltage and local power flow constraints described in (8b)–(8g). We define the auxiliary variables $\overline{U}_i$, $\overline{P}_{ik}$, $\overline{Q}_{ik}$ for the boundary conditions on the upstream bus voltages and line power flows, respectively. The global minimization problem can be formulated as follows:

$$\min_{U}\sum_{k=1}^{n}w_k\left(U_k-U^r_k\right)^2 \tag{18a}$$

such that

$$\left\{U^{(k)},\,P^{(k)},Q^{(k)}\right\}\in\mathcal{B}_k,\qquad k\in\mathcal{N}, \tag{18b}$$

and

$$U^{(k)}_i-\overline{U}_i=0,\qquad (i,k)\in\mathcal{E},\ i\neq 0, \tag{18c}$$

$$U^{(i)}_i-\overline{U}_i=0,\qquad (i,k)\in\mathcal{E},\ i\neq 0, \tag{18d}$$

$$P^{(k)}_{ik}-\overline{P}_{ik}=0,\qquad (i,k)\in\mathcal{E},\ i\neq 0, \tag{18e}$$

$$P^{(i)}_{ik}-\overline{P}_{ik}=0,\qquad (i,k)\in\mathcal{E},\ i\neq 0, \tag{18f}$$

$$Q^{(k)}_{ik}-\overline{Q}_{ik}=0,\qquad (i,k)\in\mathcal{E},\ i\neq 0, \tag{18g}$$

$$Q^{(i)}_{ik}-\overline{Q}_{ik}=0,\qquad (i,k)\in\mathcal{E},\ i\neq 0. \tag{18h}$$

$$\begin{aligned}\mathcal{L}_\rho^{(k,0)}(\cdot) = \; & w_k\left(U_k^{(k)} - U_k^r\right)^2 + \sum_{j\in\mathcal{H}_k}\left[\lambda_{kj}^v\left(\overline{U}_k - U_k^{(k)}\right) + \lambda_{kj}^p\left(\overline{P}_{kj} - P_{kj}^{(k)}\right) + \lambda_{kj}^q\left(\overline{Q}_{kj} - Q_{kj}^{(k)}\right)\right] \\ & + \frac{\rho}{2}\sum_{j\in\mathcal{H}_k}\left[\left(\overline{U}_k - U_j^{(k)}\right)^2 + \left(\overline{P}_{kj} - P_{kj}^{(k)}\right)^2 + \left(\overline{Q}_{kj} - Q_{kj}^{(k)}\right)^2\right]\end{aligned} \tag{20}$$

$$\begin{aligned}\mathcal{L}_\rho^{(k)}(\cdot) = \; & \mathcal{L}_\rho^{(k,0)}(\cdot) + \lambda_{ik}^v\left(U_i^{(k)} - \overline{U}_i\right) + \lambda_{ik}^p\left(P_{ik}^{(k)} - \overline{P}_{ik}\right) + \lambda_{ik}^q\left(Q_{ik}^{(k)} - \overline{Q}_{ik}\right) \\ & + \frac{\rho}{2}\left(U_i^{(k)} - \overline{U}_i\right)^2 + \frac{\rho}{2}\left(P_{ik}^{(k)} - \overline{P}_{ik}\right)^2 + \frac{\rho}{2}\left(Q_{ik}^{(k)} - \overline{Q}_{ik}\right)^2\end{aligned} \tag{21}$$

Note that we follow the per-phase formulation in (18) corresponding to a balanced system.

Let $\lambda_{ik}^v, \lambda_{ik}^p, \lambda_{ik}^q \in \mathbb{R}$ denote the Lagrangian multipliers associated with the equality constraints (18c)–(18d), (18e)–(18f), and (18g)–(18h), respectively. Then, the augmented Lagrangian is of the form

$$\mathcal{L}_\rho(\cdot) = \sum_{k\in\mathcal{N}} \mathcal{L}_\rho^{(k)}(\cdot), \tag{19}$$

with the $\mathcal{L}_\rho^{(k)}(\cdot)$'s defined in (20)–(21), where $\rho > 0$ is the penalty coefficient. The augmented Lagrangian given in (20) is specific for the bus directly downstream of the feeder, i.e., bus k such that $(0,k) \in \mathcal{E}$. In this particular case, there are no upstream boundary conditions on bus voltage or line power flows since the feeder voltage is fixed; consequentially, a local optimization will not be performed at the feeder. The Lagrangian for the remaining buses, as given in (21), contains additional terms for the upstream voltage and line flows of $k \in \mathcal{N}$. Then, we can cyclically optimize the augmented Lagrangian $\mathcal{L}_\rho^{(k)}(\cdot)$ with respect to one of the groups of variables, while holding the others constant with the following three-step update rule for the r^{th} iteration:

[S1.] *Local Optimization:* We take the infimum of $\mathcal{L}_\rho(\cdot)$ with respect to the primal variables, and update them as

$$U^{(k)}[r] = \underset{U^{(k)},P^{(k)},Q^{(k)}\in\mathcal{B}^{(i)}}{\arg\min}\; \mathcal{L}_\rho^{(k)}(\cdot), \tag{22}$$

which is dependent on the Lagrangian multipliers and auxiliary variables from the previous iteration $r-1$.

[S2.] *Auxilary Variable Update:* We determine the update rules for the auxiliary variables by solving

$$\nabla_{\overline{U}_i}\mathcal{L}_\rho(\cdot) = \nabla_{\overline{P}_{ik}}\mathcal{L}_\rho(\cdot) = \nabla_{\overline{Q}_{ik}}\mathcal{L}_\rho(\cdot) = 0. \tag{23}$$

The update rules for the auxiliary variables will be

$$\overline{U}_i[r] = \frac{1}{2}\left(U_i^{(k)} + U_i^{(i)}\right), \tag{24}$$

$$\overline{P}_{ik}[r] = \frac{1}{2}\left(P_{ik}^{(k)} + P_{ik}^{(i)}\right), \tag{25}$$

$$\overline{Q}_{ik}[r] = \frac{1}{2}\left(Q_{ik}^{(k)} + Q_{ik}^{(i)}\right), \tag{26}$$

for all $(i,k) \in \{\mathcal{E}\backslash(0,j)\}$.

[S3.] *Multipliers Update:* We determine the update rules for the Lagrangian multipliers by taking the gradient of $\mathcal{L}_\rho^{(k)}(\cdot)$ and utilizing a dual ascent. The update rules for multipliers will be

$$\lambda_{ik}^v[r] = \lambda_{ik}^v[r\text{-}1] + \frac{\rho}{2}\left(U_i^{(k)}[r] - U_i^{(i)}[r]\right)^{\mathrm{T}}, \tag{27a}$$

$$\lambda_{ik}^p[r] = \lambda_{ik}^p[r\text{-}1] + \frac{\rho}{2}\left(P_{ik}^{(k)}[r] - P_{ik}^{(i)}[r]\right)^{\mathrm{T}}, \tag{27b}$$

$$\lambda_{ik}^q[r] = \lambda_{ik}^q[r\text{-}1] + \frac{\rho}{2}\left(Q_{ik}^{(k)}[r] - Q_{ik}^{(i)}[r]\right)^{\mathrm{T}}. \tag{27c}$$

Note that in Step S3, we use a single dual variable for each boundary condition on a distribution line segment rather than two (one for each subproblem) and account for this through a sign difference between upstream and downstream buses.

V. Case Studies

In this section, we illustrate the ability of the QP-based OPF to optimally track some reference voltage. We begin by formulating the SDP-based OPF that will be used as a baseline comparison for the QP-based OPF, since it captures the nonlinearities of the power flow equations. Then, we demonstrate the ability of the QP-based OPF to regulate the system voltages to the voltage profile determined by the slow time-scale optimization proposed in [3] with a 15-bus unbalanced three-phase distribution system. We performed the simulations in MATLAB using the CVX package [23], which was employed to solve the centralized problem and to update the primal variables $\boldsymbol{U}, \boldsymbol{P}, \boldsymbol{Q}$ in Step S1 of the distributed algorithm. Finally, we extend results to a 123-bus unbalanced three-phase distribution system. In each of the simulations, we treat the reference voltages $\boldsymbol{V}^r$ as a known quantity that was determined with the OPF-based method for dispatching slow time-scale actuators proposed in [3]; this method provides a solution that minimizes the voltage deviations from 1 p.u. at the rated load while enforcing that the bus voltages are within $[0.95, 1.05]$ p.u.

A. SDP-Based Voltage Regulation

We will compare the proposed optimization in Section III against the SDP-based OPF in [3] adapted for the unbalanced voltage regulation problem. As noted earlier, we do not compare against an SOCP-based OPF, since the results in this section are for unbalanced three-phase systems, and we do not consider balanced systems. The SDP-based OPF will have the form

$$\min_{\boldsymbol{W}\succeq\boldsymbol{0}}\; f_0\left(\boldsymbol{W}\right) + \sum_{k\in\mathcal{N}}\left\|\boldsymbol{w}_k \odot \left(\boldsymbol{U}_k^r - \mathrm{diag}\left(\boldsymbol{W}_{kk}\right)\right)\right\|^2 \tag{28a}$$

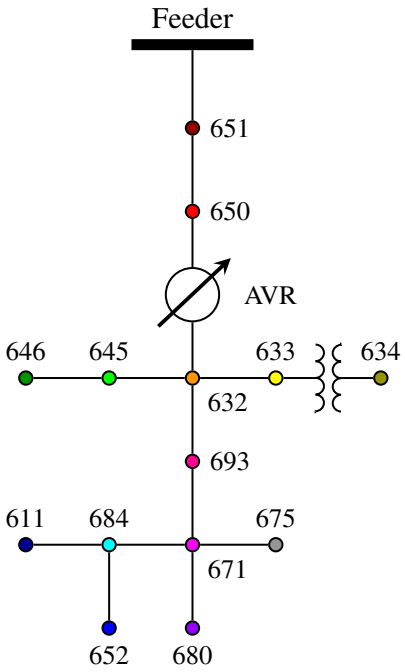

Figure 4: 15-bus unbalanced distribution system.

such that, for all $i \in \{a, b, c\}$,

$$\boldsymbol{U}_0 - |\boldsymbol{V}^s| \odot |\boldsymbol{V}^s| = 0, \tag{28b}$$

$$\text{Tr}\,(H_{k_i}\boldsymbol{W}) - \boldsymbol{S}_{k_i} - j\boldsymbol{q}_{k_i} = 0, \quad \forall k \in \mathcal{N}_c, \tag{28c}$$

$$\text{Tr}\,(H_{k_i}\boldsymbol{W}) - \boldsymbol{S}_{k_i} = 0, \quad \forall k \in \mathcal{N}_u, \tag{28d}$$

and

$$\underline{V}^2 \leq [\boldsymbol{W}]_{k_i k_i} \leq \overline{V}^2, \quad \forall k \in \mathcal{N}, \tag{28e}$$

$$\underline{\boldsymbol{q}}_k \leq \quad \boldsymbol{q}_k \quad \leq \overline{\boldsymbol{q}}_k, \quad \forall k \in \mathcal{N}_c, \tag{28f}$$

where $\boldsymbol{W} = \boldsymbol{V}\boldsymbol{V}^H \in \mathbb{C}^{3(n+1)\times 3(n+1)}$ is the outer product of the bus voltage with its conjugate, $f_0(\boldsymbol{W})$ is the distribution line segment active power losses,[1] $\boldsymbol{W}_{kk} \in \mathbb{C}^{3\times 3}$ is the sub-matrix associated with bus k, and $\text{Tr}\,(H_{k_i}\boldsymbol{W})$ is the complex power flow equation for phase i of bus k.

B. 15-Bus Unbalanced Three-Phase Results

We begin with the 15-bus network shown in Fig. 4, which we derived from the IEEE 13-bus—an unbalanced three-phase distribution system, (see, e.g., [22], [24]). The system has a three-phase voltage regulation transformer between buses 650 and 632. The rest of the system contains single-, two-, and three-phase sublaterals. Buses 650 and 651 were added between the feeder and the transformer, so that the transformer was not directly connected to the feeder. Bus 693 was added to account for the distributed load along line $(632, 671)$, and bus 692 was removed, since it corresponds to a closed switch connected between buses 671 and 675. In all of the simulations, the feeder is balanced with a voltage magnitude of 1.03 p.u. Note that the color coding of the buses in Fig. 4 correspond to the system response curves in Figs. 5, 7, and 8.

[1]Note that the objective function of the SDP-based OPF requires the line loss term $f_0(\boldsymbol{W})$ to perform the rank relaxation [3].

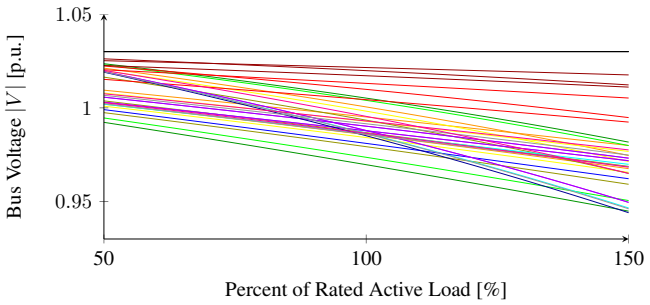

(a) Uncontrolled voltage response.

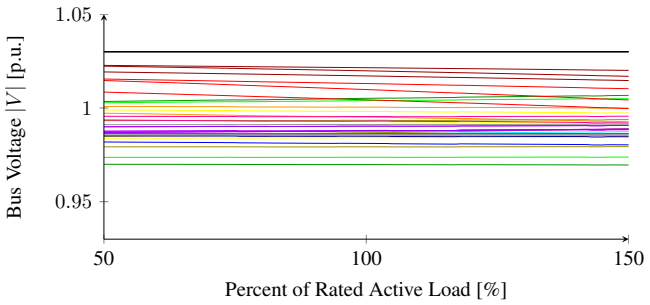

(b) SDP-based controlled voltage response.

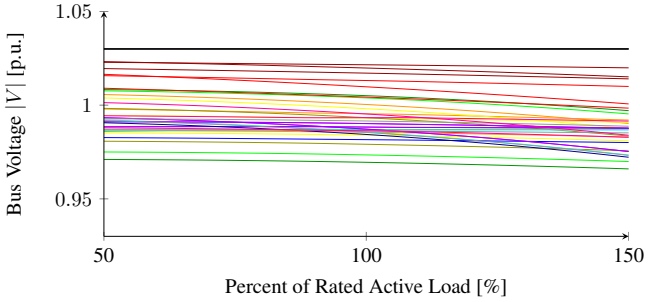

(c) QP-based controlled voltage response.

Figure 5: SDP-based optimal control of bus voltage magnitudes with reactive power support.

The loads will naturally vary over time, but we are particularly interested in variations of active power injection (positive or negative), due to renewable-based generation and uncontrolled load from storage-capable devices (e.g., PHEV). In the simulations, we hold the reactive power constant and uniformly vary the active power from 50% to 150% of the rated load at each bus. For simplicity, we assume that the network has a large penetration of DERs with reactive power provision capabilities, and that the reactive power limits $\underline{q}_k$, $\overline{q}_k$ are on the same order of magnitude as the bus loads. Figure 5 shows the voltage responses for the uncontrolled case, the SDP-based OPF, and the QP-based OPF where the nonlinear terms are treated as constants, as described in Section III-C. The uncontrolled voltage responses shown in Fig. 5(a) has a minimum voltage of 0.97 p.u. at rated load that drops to 0.944 p.u. at maximum loading, which is outside of the desired 1 ± 0.5 p.u. operating criterion for bus voltages. The SDP-based OPF in Fig. 5(b) improves the voltage response significantly, with most buses maintaining their reference voltages. Lastly,

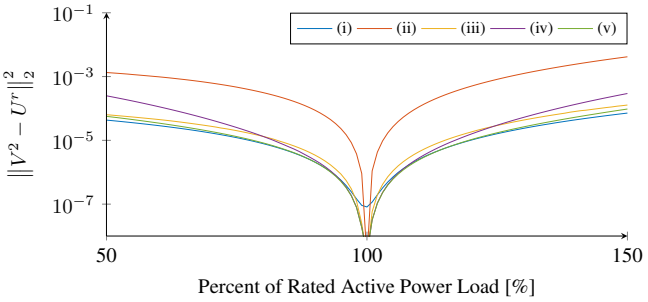

Figure 6: Relative costs for each control method.

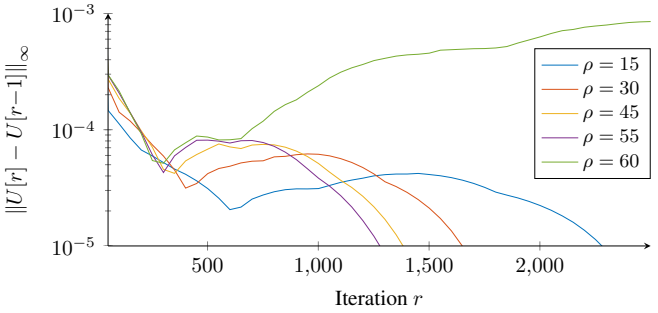

Figure 7: Impacts of the choice of the penalty parameter ρ.

the QP-based OPF is shown in Fig. 5(c) with the lowest voltage dropping from 0.97 p.u. to 0.966 p.u.

While the SDP-based approach has an advantage over the QP-based approach in a wider range of operating points, we have shown that the QP-based OPF will produce similar results with less of a computational burden. In the 15-bus system, there are 38 unique phases to track (not every bus has all three phases), so the SDP-based OPF will have approximately 5200 optimization variables with a positive semidefinite constraint on $\boldsymbol{W}$. Also, the number of variables will grow exponentially with respect to the number of buses. The method proposed in this paper will have approximately 150 optimization variables and grows linearly.

1) Nonlinear Loss Term Approximations: In Section III-A, we mentioned that we can improve the accuracy of the linear model with a linear curve to approximate the nonlinear terms (rather than treat them as constants), and/or recompute the constants/coefficients based on the measured power flows. Next, we compare the accuracy of the linear approximation using these techniques. Figure 6 shows the ability of the fast time-scale optimizations to regulate bus voltages with the active power uniformly swept from 50% to 150% of rated load. The curves represent the following:

(i) This curve shows the results using the SDP-based OPF described in (28). This approach represents the base case to compare against, since it considers the nonlinear system.

(ii) The results for the OPF described in (8), where we compute the constants $\boldsymbol{c}_{ik}^u(\boldsymbol{P}_o, \boldsymbol{Q}_o)$, $\boldsymbol{c}_{ik}^p(\boldsymbol{P}_o, \boldsymbol{Q}_o)$, and $\boldsymbol{c}_{ik}^q(\boldsymbol{P}_o, \boldsymbol{Q}_o)$ based on the initial operating point $(\boldsymbol{P}_o, \boldsymbol{Q}_o, \boldsymbol{V}^r)$ determined by the slow time-scale control.

(iii) In this case, we recompute constants based on the measured power flows $(\boldsymbol{P}, \boldsymbol{Q})$ and the desired reference voltage $\boldsymbol{V}^r$.

(iv) This curve represents the first-order approximation of the system losses that we described in (6) with fixed coefficients, where $\boldsymbol{c}_{ik}^u(\boldsymbol{P}_o, \boldsymbol{Q}_o)$, $\boldsymbol{c}_{ik}^p(\boldsymbol{P}_o, \boldsymbol{Q}_o)$, and $\boldsymbol{c}_{ik}^q(\boldsymbol{P}_o, \boldsymbol{Q}_o)$ are a function of the line flows and initialized based on the slow time-scale dispatch.

(v) In this optimization, we combine the concepts in (iii)–(iv) and we reinitialize the coefficients of the linear approximation based on the current operating conditions $(\boldsymbol{P}, \boldsymbol{Q})$ and the reference voltage $\boldsymbol{V}^r$.

The nonlinear SDP-based OPF in (i) provides a lower bound with the constants in (ii) behaving as an upper bound for cost functions of the optimizations. The first-order approximation in (iv) does improve the solution compared to estimating $\boldsymbol{c}_{ik}^u(\boldsymbol{P}, \boldsymbol{Q})$, $\boldsymbol{c}_{ik}^p(\boldsymbol{P}, \boldsymbol{Q})$, and $\boldsymbol{c}_{ik}^q(\boldsymbol{P}, \boldsymbol{Q})$ as constants (ii); however, updating the system model based on the current operating conditions improves the accuracy of the linear system models in (iii) and (v) dramatically.

2) ADMM-Based Distributed Solution: Next, we perform a single optimization with the distributed algorithm described in Section IV on the 15-bus unbalanced three-phase distribution system. As we stated earlier, the distributed optimization scheme is designed to leverage the communication infrastructure from the slow time-scale optimization in [3]. In this case, each partition contains a single bus and our stopping criteria will be

$$\|\boldsymbol{U}[r] - \boldsymbol{U}[r-1]\|_\infty < \varepsilon, \tag{29}$$

where we continue to run the distributed algorithm until the last bus voltage converges to within the tolerance ε [p.u.]. We found that $\varepsilon = 1\text{e}{-5}$ p.u. was an appropriate choice in terms of speed and accuracy. Furthermore, we update $\boldsymbol{c}_{ik}^u(\boldsymbol{P}, \boldsymbol{Q})$, $\boldsymbol{c}_{ik}^p(\boldsymbol{P}, \boldsymbol{Q})$, and $\boldsymbol{c}_{ik}^q(\boldsymbol{P}, \boldsymbol{Q})$ relative to the current operating conditions, since these are known quantities that are sampled.

For this simulation, we initialized the reference voltage with the rated loads. Then, we created an under-voltage situation by increasing the system loads to 130% of their rated values, which drops the lowest bus voltage from 0.970 to 0.938 p.u. Figure 7 and Table I show the convergence results for several values of ρ. The system converged the fastest for $\rho = 55$; however, increasing the penalty parameter to $\rho = 60$ caused the algorithm to diverge. Figure 8 shows the evolution of the distributed optimization for $\rho = 55$ with the local augmented Lagrangians in Fig. 8(a) and the bus voltages

Table I: CONVERGENCE OF THE DISTRIBUTED ALGORITHM

ρ	Iterations	$\|\boldsymbol{V}^2\text{-}\boldsymbol{U}^r\|_2^2$
15	2281	3.0e-3
30	1650	1.7e-3
45	1383	1.0e-3
55	1278	7.6e-4
60	-	-

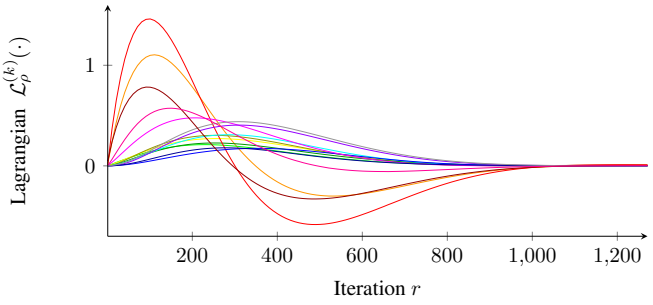

(a) Local Lagrangians at each bus for $\rho = 55$.

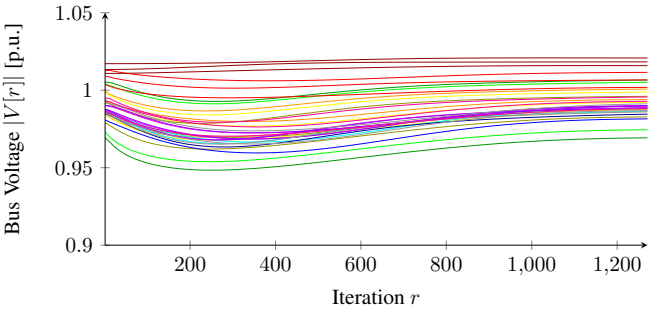

(b) Voltage magnitudes $\rho = 55$.

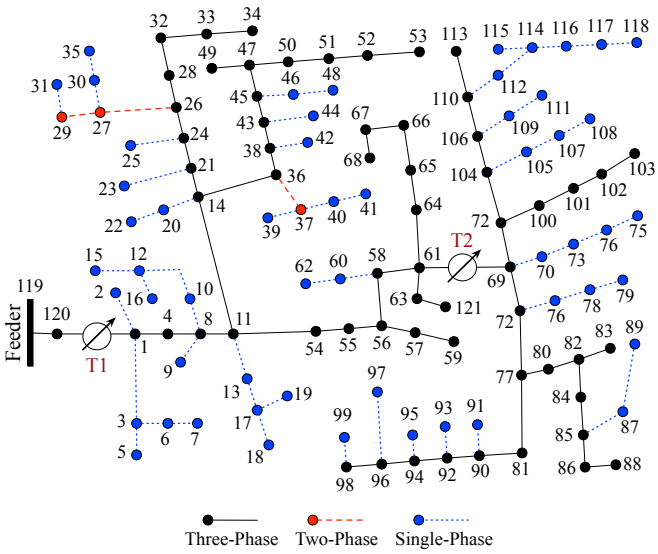

Figure 9: 123-bus unbalanced distribution system.

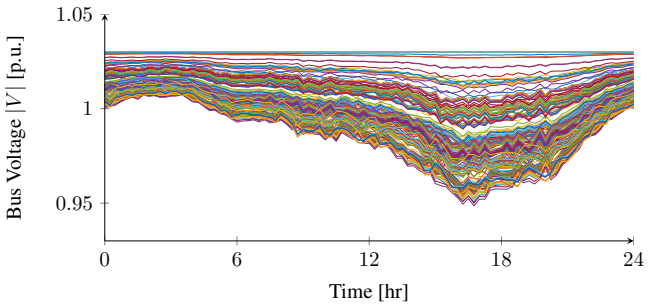

(a) Uncontrolled voltage response.

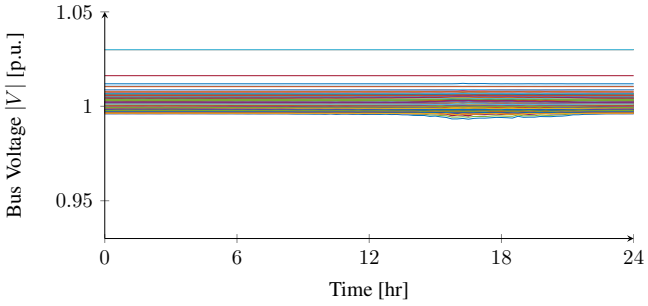

(b) Controlled voltage response.

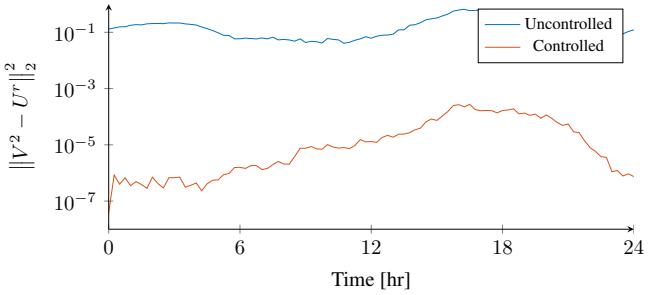

(c) Voltage error from reference voltage.

Figure 10: 123-bus system responses.

in Fig. 8(b). The cost function for the distributed algorithm returned results that were on the same order of magnitude as those obtained with the centralized solvers in Section III. We already demonstrated that the SDP-based approach scales exponentially with the system size and the QP-based OPF will scale linearly; however, the key advantage of the distributed solver is that the complexity of the local problem is dependent on the partition size and not the system size. We refer the reader to [10], [20], [21] for computational benefits of ADMM.

C. 123-Bus Unbalanced Three-phase Results

In this section, we demonstrate the ability of the QP-based OPF to scale up to the modified IEEE 123-bus test system [24] shown in Fig. 9, where we removed the fixed shunt capacitors and the two voltage regulators that were not three phase. We developed a load curve based distribution-level load data from [25], which offers datasets on commercial and residential energy consumption. Similar to the 15-bus network, we initialized the system with a slow time-scale optimization and hold the transformer constant for the duration of the simulation. It is assumed that reactive power support available at each load bus is on the order of the rated load.

Figure 10(a) shows the uncontrolled voltage response where the voltage magnitude drops slightly outside specification around 17:00 hours. The controlled response with the QP-based OPF is shown ing Fig. 10(b). Intuitively, the voltage magnitudes dip during the peak evening load, but the error from the reference voltage $\boldsymbol{V}^r$ is significantly reduced, as shown by Fig. 10(c). Given sudden or significant changes in the system load, it follows naturally that we would redispatch the system resources with the slow time-scale OPF, e.g., during the 16:00-22:00 hour time period; however, it is a nontrivial task to blend the two time-scales, and we intend to pursue this

concept in future work.

VI. Concluding Remarks

In this paper, we developed a method to optimally regulate bus voltages for unbalanced distribution systems via a convex quadratic optimization program. We showed the potential of the proposed method and ADMM-based algorithm with a 15-bus unbalanced three-phase distribution system.

Future work will include coupling the proposed voltage regulation scheme with the slow time-scale control proposed in [3], to showcase a system-wide control method that accounts for the fast regulation required to mitigate voltage deviations associated with the uncontrolled generation/consumption by DERs and to dispatch existing hardware on a slower time-scale.

Appendix

A. Approximate Phase Imbalances of the Voltage Constraints

In Section III-C, we assume that the phases are nearly balanced with respect to each other in the assumptions described by (10) and (11), which we use to derive the approximate distribution line segment impedances in (12)–(15) for the three-phase case. In this appendix, we apply a similar approach as we will use in Appendix B to approximate the imbalances of the phases on bus i.

First, we retain the assumption that the voltage magnitudes of the phases at bus i are similar, e.g., $|V_{i_a}| \approx |V_{i_b}| \approx |V_{i_c}|$. Next, we measure the phase angles relative to θ_{i_a} to determine $(\tilde{\theta}_{i_b}, \tilde{\theta}_{i_c})$, which we can perform based on the current operating conditions or at the time of the slow time-scale dispatch. Thus, we update (13)–(15) to be

$$\boldsymbol{a}_i = \begin{bmatrix} 1 & e^{j\tilde{\theta}_{i_b}} & e^{j\tilde{\theta}_{i_c}} \end{bmatrix}^{\mathrm{T}}, \tag{30}$$

$$\tilde{\boldsymbol{r}}_{ik} = \mathrm{Re}\left\{\boldsymbol{a}_i \boldsymbol{a}_i^{\mathrm{H}}\right\} \odot \boldsymbol{r}_{ik} + \mathrm{Im}\left\{\boldsymbol{a}_i \boldsymbol{a}_i^{\mathrm{H}}\right\} \odot \boldsymbol{x}_{ik}, \tag{31}$$

$$\tilde{\boldsymbol{x}}_{ik} = \mathrm{Re}\left\{\boldsymbol{a}_i \boldsymbol{a}_i^{\mathrm{H}}\right\} \odot \boldsymbol{x}_{ik} - \mathrm{Im}\left\{\boldsymbol{a}_i \boldsymbol{a}_i^{\mathrm{H}}\right\} \odot \boldsymbol{r}_{ik}, \tag{32}$$

for all $(i,k) \in \mathcal{E}$.

B. Unbalanced Three-Phase Linear Approximation

This appendix provides the derivation of the linear approximation of the nonlinear elements of the unbalanced three-phase optimization problem formulated in Section III-C. First, we define $\bar{\boldsymbol{a}}_i \in \mathbb{C}^3$ to represent the element-wise inverse voltage of bus i. We can use three approaches to approximate $\bar{\boldsymbol{a}}_i$ in the unbalanced three-phase case, (i) treat $\bar{\boldsymbol{a}}_i$ as a constant, which is the approach we took in Section III-C, (ii) we can assume that the phases are nearly balanced and update $\bar{\boldsymbol{a}}_i$ based on $\boldsymbol{V}_i^r$, or (iii) recompute $\bar{\boldsymbol{a}}_i$ at each optimization based on the measure phase angles $(\theta_{i_a}, \theta_{i_b}, \theta_{i_c})$ and $\boldsymbol{V}_i^r$. Thus, $\bar{\boldsymbol{a}}_i$ as described in (ii) will be

$$\bar{\boldsymbol{a}}_i = \begin{bmatrix} 1 & e^{j2\pi/3} & e^{-j2\pi/3} \end{bmatrix}^{\mathrm{T}} \oslash \boldsymbol{V}_i^r,$$

when we assume that the phases at each bus are approximately balanced. Similarly, for the case in (iii), $\bar{\boldsymbol{a}}_i$ is given by

$$\bar{\boldsymbol{a}}_i = \begin{bmatrix} e^{-j\theta_{i_a}} & e^{-j\theta_{i_b}} & e^{-j\theta_{i_c}} \end{bmatrix}^{\mathrm{T}} \oslash \boldsymbol{V}_i^r,$$

where we update $\bar{\boldsymbol{a}}_i$ based on the current reference voltage and the measure phase angles.

1) Nonlinear Voltage Drop Term: The nonlinear term in the voltage drop equation is

$$\begin{aligned} \boldsymbol{c}_{ik}^u(\boldsymbol{P},\boldsymbol{Q}) &= \left[\boldsymbol{z}_{ik}\left[\boldsymbol{S}_{ik}^* \oslash \boldsymbol{V}_i^*\right]\right] \odot \left[\boldsymbol{z}_{ik}^*\left[\boldsymbol{S}_{ik_o} \oslash \boldsymbol{V}_i\right]\right], \\ &\approx \left[\boldsymbol{z}_{ik}\left[\boldsymbol{S}_{ik}^* \odot \bar{\boldsymbol{a}}_i^*\right]\right] \odot \left[\boldsymbol{z}_{ik}^*\left[\boldsymbol{S}_{ik_o} \oslash \bar{\boldsymbol{a}}_i\right]\right]. \end{aligned} \tag{33}$$

Let the updated distribution line segment impedance be

$$\bar{\boldsymbol{z}}_{ik} = \boldsymbol{z}_{ik}\,\mathrm{diag}\left(\bar{\boldsymbol{a}}_i^*\right) = \bar{\boldsymbol{r}}_{ik} + j\bar{\boldsymbol{x}}_{ik}. \tag{34}$$

Then, (33) will become

$$\begin{aligned} \boldsymbol{c}_{ik}^u(\boldsymbol{P},\boldsymbol{Q}) = {} & [\bar{\boldsymbol{r}}_{ik}\boldsymbol{P}_{ik}] \odot [\bar{\boldsymbol{r}}_{ik}\boldsymbol{P}_{ik}] + [\bar{\boldsymbol{x}}_{ik}\boldsymbol{Q}_{ik}] \odot [\bar{\boldsymbol{x}}_{ik}\boldsymbol{Q}_{ik}] \\ & + [\bar{\boldsymbol{x}}_{ik}\boldsymbol{P}_{ik}] \odot [\bar{\boldsymbol{x}}_{ik}\boldsymbol{P}_{ik}] + [\bar{\boldsymbol{r}}_{ik}\boldsymbol{Q}_{ik}] \odot [\bar{\boldsymbol{r}}_{ik}\boldsymbol{Q}_{ik}] \\ & + 2\left[\bar{\boldsymbol{r}}_{ik}\boldsymbol{P}_{ik}\right] \odot \left[\bar{\boldsymbol{x}}_{ik}\boldsymbol{Q}_{ik}\right] \\ & - 2\left[\bar{\boldsymbol{x}}_{ik}\boldsymbol{P}_{ik}\right] \odot \left[\bar{\boldsymbol{r}}_{ik}\boldsymbol{Q}_{ik}\right]. \end{aligned} \tag{35}$$

The linear approximation of (35) around the point $(\boldsymbol{P}_o, \boldsymbol{Q}_o)$ is given by

$$\begin{aligned} \boldsymbol{c}_{ik}^u(\boldsymbol{P},\boldsymbol{Q}) \approx {} & f_{p_{ik}}(\boldsymbol{P}_o,\boldsymbol{Q}_o)\left[\boldsymbol{P}_{ik} - \boldsymbol{P}_{ik_o}\right] + \\ & f_{q_{ik}}(\boldsymbol{P}_o,\boldsymbol{Q}_o)\left[\boldsymbol{Q}_{ik} - \boldsymbol{Q}_{ik_o}\right] + \boldsymbol{c}_{ik}^u(\boldsymbol{P}_o,\boldsymbol{Q}_o), \end{aligned} \tag{36}$$

where the partial derivatives are

$$\begin{aligned} f_{p_{ik}} = \frac{\partial \boldsymbol{c}_{ik}^u}{\partial \boldsymbol{P}_{ik}} = {} & h_{xx}\left(\bar{\boldsymbol{r}}_{ik}, \boldsymbol{P}_{ik}\right) + h_{xx}\left(\bar{\boldsymbol{x}}_{ik}, \boldsymbol{P}_{ik}\right) \\ & + 2h_{xy}\left(\bar{\boldsymbol{r}}_{ik}, \bar{\boldsymbol{x}}_{ik}, \boldsymbol{P}_{ik}, \boldsymbol{Q}_{ik}\right) \\ & - 2h_{xy}\left(\bar{\boldsymbol{x}}_{ik}, \bar{\boldsymbol{r}}_{ik}, \boldsymbol{P}_{ik}, \boldsymbol{Q}_{ik}\right), \\ f_{q_{ik}} = \frac{\partial \boldsymbol{c}_{ik}^u}{\partial \boldsymbol{Q}_{ik}} = {} & h_{xx}\left(\bar{\boldsymbol{r}}_{ik}, \boldsymbol{Q}_{ik}\right) + h_{xx}\left(\bar{\boldsymbol{x}}_{ik}, \boldsymbol{Q}_{ik}\right) \\ & + 2h_{xy}\left(\bar{\boldsymbol{x}}_{ik}, \bar{\boldsymbol{r}}_{ik}, \boldsymbol{Q}_{ik}, \boldsymbol{P}_{ik}\right) \\ & - 2h_{xy}\left(\bar{\boldsymbol{r}}_{ik}, \bar{\boldsymbol{x}}_{ik}, \boldsymbol{Q}_{ik}, \boldsymbol{P}_{ik}\right), \end{aligned}$$

and

$$\begin{aligned} h_{xx}\left(\boldsymbol{A}, \boldsymbol{x}\right) &= 2\boldsymbol{A}\,\mathrm{diag}\left(\boldsymbol{A}\boldsymbol{x}\right), \\ h_{xy}\left(\boldsymbol{A}, \boldsymbol{B}, \boldsymbol{x}, \boldsymbol{y}\right) &= \boldsymbol{A}\,\mathrm{diag}\left(\boldsymbol{B}\boldsymbol{y}\right). \end{aligned}$$

2) Nonlinear Power Loss Terms: The power loss across the distribution line segment $(i,k) \in \mathcal{E}$ is given by

$$\boldsymbol{S}_{ik}^{\ell} = \left[\boldsymbol{S}_{ik} \oslash \boldsymbol{V}_i\right] \odot \left[\boldsymbol{z}_{ik}\left(\boldsymbol{S}_{ik}^* \oslash \boldsymbol{V}_i^*\right)\right]. \tag{37}$$

We update the distribution line segment impedance to be

$$\hat{\boldsymbol{z}}_{ik} = \hat{\boldsymbol{r}}_{ik} + j\hat{\boldsymbol{x}}_{ik} = \boldsymbol{z}_{ik} \odot \left(\bar{\boldsymbol{a}}_i \bar{\boldsymbol{a}}_i^{\mathrm{H}}\right), \tag{38}$$

such that

$$\hat{\boldsymbol{r}}_{ik} = \mathrm{Re}\left\{\bar{\boldsymbol{a}}_i \bar{\boldsymbol{a}}_i^{\mathrm{H}}\right\} \odot \boldsymbol{r}_{ik} - \mathrm{Im}\left\{\bar{\boldsymbol{a}}_i \bar{\boldsymbol{a}}_i^{\mathrm{H}}\right\} \odot \boldsymbol{x}_{ik}, \tag{39}$$

$$\hat{\boldsymbol{x}}_{ik} = \mathrm{Re}\left\{\bar{\boldsymbol{a}}_i \bar{\boldsymbol{a}}_i^{\mathrm{H}}\right\} \odot \boldsymbol{x}_{ik} + \mathrm{Im}\left\{\bar{\boldsymbol{a}}_i \bar{\boldsymbol{a}}_i^{\mathrm{H}}\right\} \odot \boldsymbol{r}_{ik}. \tag{40}$$

Thus, we can rewrite (37) as

$$\boldsymbol{S}_{ik}^{\ell} = \left[\boldsymbol{P}_{ik} + j\boldsymbol{Q}_{ik}\right] \odot \left[\hat{\boldsymbol{z}}_{ik}\left(\boldsymbol{P}_{ik} - j\boldsymbol{Q}_{ik}\right)\right], \tag{41}$$

where we separate the active and reactive power losses along the distribution line segment to compute the nonlinear power loss terms

$$\begin{aligned} \boldsymbol{c}_{ik}^p(\boldsymbol{P},\boldsymbol{Q}) = {} & \boldsymbol{P}_{ik} \odot \left[\hat{\boldsymbol{r}}_{ik}\boldsymbol{P}_{ik} + \hat{\boldsymbol{x}}_{ik}\boldsymbol{Q}_{ik}\right] \\ & + \boldsymbol{Q}_{ik} \odot \left[\hat{\boldsymbol{r}}_{ik}\boldsymbol{Q}_{ik} - \hat{\boldsymbol{x}}_{ik}\boldsymbol{P}_{ik}\right], \end{aligned} \tag{42}$$

and

$$\begin{aligned}\boldsymbol{c}^q_{ik}(\boldsymbol{P},\boldsymbol{Q}) = \boldsymbol{P}_{ik} \odot [\hat{\boldsymbol{x}}_{ik}\boldsymbol{P}_{ik} - \hat{\boldsymbol{r}}_{ik}\boldsymbol{Q}_{ik}] \\ + \boldsymbol{Q}_{ik} \odot [\hat{\boldsymbol{r}}_{ik}\boldsymbol{P}_{ik} + \hat{\boldsymbol{x}}_{ik}\boldsymbol{Q}_{ik}],\end{aligned} \tag{43}$$

respectively. The linear approximate of (42) and (43) will be

$$\begin{aligned}\boldsymbol{c}^p_{ik}(\boldsymbol{P},\boldsymbol{Q}) \approx\ & f_{p_{ik}}(\boldsymbol{P}_o,\boldsymbol{Q}_o)\,[\boldsymbol{P}_{ik}-\boldsymbol{P}_{ik_o}]+ \\ & f_{q_{ik}}(\boldsymbol{P}_o,\boldsymbol{Q}_o)\,\left[\boldsymbol{Q}_{ik}-\boldsymbol{Q}_{ik_o}\right]+\boldsymbol{c}^p_{ik}(\boldsymbol{P}_o,\boldsymbol{Q}_o),\end{aligned} \tag{44}$$

and

$$\begin{aligned}\boldsymbol{c}^q_{ik}(\boldsymbol{P},\boldsymbol{Q}) \approx\ & g_{p_{ik}}(\boldsymbol{P}_o,\boldsymbol{Q}_o)\,[\boldsymbol{P}_{ik}-\boldsymbol{P}_{ik_o}]+ \\ & g_{q_{ik}}(\boldsymbol{P}_o,\boldsymbol{Q}_o)\,\left[\boldsymbol{Q}_{ik}-\boldsymbol{Q}_{ik_o}\right]+\boldsymbol{c}^q_{ik}(\boldsymbol{P}_o,\boldsymbol{Q}_o),\end{aligned} \tag{45}$$

where the partial derivatives are

$$\begin{aligned}f_{p_{ik}} = \frac{\partial \boldsymbol{c}^p_{ik}}{\partial \boldsymbol{P}_{ik}} &= h_{xx}\left(\hat{\boldsymbol{r}}_{ik},\boldsymbol{P}_{ik}\right) + h_{xy}\left(\hat{\boldsymbol{x}}_{ik},\boldsymbol{P}_{ik},\boldsymbol{Q}_{ik}\right) \\ &\quad - h_{yx}\left(\hat{\boldsymbol{x}}_{ik},\boldsymbol{Q}_{ik},\boldsymbol{P}_{ik}\right), \\ f_{q_{ik}} = \frac{\partial \boldsymbol{c}^p_{ik}}{\partial \boldsymbol{Q}_{ik}} &= h_{xx}\left(\hat{\boldsymbol{r}}_{ik},\boldsymbol{Q}_{ik}\right) - h_{xy}\left(\hat{\boldsymbol{x}}_{ik},\boldsymbol{Q}_{ik},\boldsymbol{P}_{ik}\right) \\ &\quad + h_{yx}\left(\hat{\boldsymbol{x}}_{ik},\boldsymbol{P}_{ik},\boldsymbol{Q}_{ik}\right), \\ g_{p_{ik}} = \frac{\partial \boldsymbol{c}^q_{ik}}{\partial \boldsymbol{P}_{ik}} &= h_{xx}\left(\hat{\boldsymbol{x}}_{ik},\boldsymbol{P}_{ik}\right) - h_{xy}\left(\hat{\boldsymbol{r}}_{ik},\boldsymbol{P}_{ik},\boldsymbol{Q}_{ik}\right) \\ &\quad + h_{yx}\left(\hat{\boldsymbol{r}}_{ik},\boldsymbol{Q}_{ik},\boldsymbol{P}_{ik}\right), \\ g_{q_{ik}} = \frac{\partial \boldsymbol{c}^q_{ik}}{\partial \boldsymbol{Q}_{ik}} &= h_{xx}\left(\hat{\boldsymbol{x}}_{ik},\boldsymbol{Q}_{ik}\right) + h_{xy}\left(\hat{\boldsymbol{r}}_{ik},\boldsymbol{Q}_{ik},\boldsymbol{P}_{ik}\right) \\ &\quad + h_{yx}\left(\hat{\boldsymbol{r}}_{ik},\boldsymbol{P}_{ik},\boldsymbol{Q}_{ik}\right),\end{aligned}$$

and

$$\begin{aligned}h_{xx}\left(\boldsymbol{A},\boldsymbol{x}\right) &= \operatorname{diag}\left(\boldsymbol{A}\boldsymbol{x}\right) + \operatorname{diag}\left(\boldsymbol{x}\right)\boldsymbol{A}, \\ h_{xy}\left(\boldsymbol{A},\boldsymbol{x},\boldsymbol{y}\right) &= \operatorname{diag}\left(\boldsymbol{A}\boldsymbol{y}\right), \\ h_{yx}\left(\boldsymbol{A},\boldsymbol{x},\boldsymbol{y}\right) &= \operatorname{diag}\left(\boldsymbol{x}\right)\boldsymbol{A}.\end{aligned}$$

REFERENCES

[1] B. A. Robbins, A. D. Dominguez-Garcia, and C. N. Hadjicostis, "Control of distributed energy resources for reactive power support," in *Proc. of 2011 North American Power Symposium (NAPS)*, 2011, pp. 1–5.

[2] "IEEE application guide for IEEE Std 1547, IEEE standard for interconnecting distributed resources with electric power systems," *IEEE Std. 1547.2-2008*, pp. 1–207, Apr. 2009.

[3] B. A. Robbins, H. Zhu, and A. D. Domínguez-García, "Optimal tap setting of voltage regulation transformers in unbalanced distribution systems," *IEEE Trans. on Power Systems*, to appear.

[4] K. Turitsyn, P. Šulc, S. Backhaus, and M. Chertkov, "Distributed control of reactive power flow in a radial distribution circuit with high photovoltaic penetration," in *Proc. of IEEE Power and Energy Society General Meeting*, Jul. 2010, pp. 1–6.

[5] M. Baran and F. Wu, "Optimal capacitor placement on radial distribution systems," *IEEE Trans. on Power Delivery*, vol. 4, no. 1, pp. 725–734, Jan. 1989.

[6] ——, "Optimal sizing of capacitors placed on a radial distribution system," *IEEE Trans. on Power Delivery*, vol. 4, no. 1, pp. 735–743, Jan. 1989.

[7] D. Wang, K. Turitsyn, and M. Chertkov, "Distflow ode: Modeling, analyzing and controlling long distribution feeder," in *Proc. of IEEE Conf. on Decision and Control (CDC)*, Dec. 2012, pp. 5613–5618.

[8] P. Šulc, S. Backhaus, and M. Chertkov, "Optimal distributed control of reactive power via the alternating direction method of multipliers," *IEEE Trans. on Energy Conversion*, vol. 29, no. 4, pp. 968–977, Dec. 2014.

[9] L. Gan and S. H. Low, "Convex relaxations and linear approximation for optimal power flow in multiphase radial networks," [Available]: arXiv:1406.3054, Jun. 2014.

[10] S. Boyd, N. Parikh, E. Chu, B. Peleato, and J. Eckstein, "Distributed optimization and statistical learning via the alternating direction method of multipliers," *Foundations and Trends in Machine Learning*, vol. 3, no. 1, pp. 1–122, 2011.

[11] M. Farivar and S. H. Low, "Branch flow model: Relaxations and convexification," *IEEE Trans. on Power Systems*, vol. 28, no. 3, pp. 2554–2564, Aug. 2013.

[12] Q. Peng and S. H. Low, "Distributed algorithm for optimal power flow on a radial network," [Available]: arXiv:1404.0700, Apr. 2014.

[13] J. Lavaei and S. H. Low, "Zero duality gap in optimal power flow problem," *IEEE Trans. on Power Systems*, vol. 27, no. 1, pp. 92–107, 2012.

[14] B. Zhang, A. Lam, A. Domínguez-García, and D. Tse, "An optimal and distributed method for voltage regulation in power distribution systems," *IEEE Trans. on Power Systems*, to appear.

[15] E. Dall'Anese, S. Dhople, and G. B. Giannakis, "Optimal dispatch of photovoltaic inverters in residential distribution systems," *IEEE Trans. on Sustainable Energy*, vol. 5, no. 2, pp. 487–497, Apr. 2014.

[16] J. Lavaei, D. Tse, and B. Zhang, "Geometry of power flows in tree networks," in *Proc. of IEEE Power and Energy Society General Meeting*, 2012, pp. 1–8.

[17] S. Bose, D. F. Gayme, S. H. Low, and K. M. Chandy, "Optimal power flow over tree networks," in *Proc. of Allerton Conf. on Comm., Control, & Computing*, 2011, pp. 1342–1348.

[18] B. A. Robbins, C. N. Hadjicostis, and A. D. Dominguez-Garcia, "A two-stage distributed architecture for voltage control in power distribution systems," *IEEE Trans. on Power Systems*, vol. 28, no. 2, pp. 1470–1482, May 2013.

[19] B. Zhang, A. D. Domínguez-García, and D. Tse, "A local control approach to voltage regulation in distribution networks," in *Proc. of North American Power Symposium*, Sep. 2013, pp. 1–6.

[20] E. Dall'Anese, H. Zhu, and G. Giannakis, "Distributed optimal power flow for smart microgrids," *IEEE Trans. on Smart Grid*, vol. 4, no. 3, pp. 1464–1475, Sep. 2013.

[21] M. Kraning, E. Chu, J. Lavaei, and S. Boyd, "Dynamic network energy management via proximal message passing," *Foundations and Trends in Optimization*, vol. 1, no. 2, pp. 1–54, 2013.

[22] W. H. Kersting, *Distribution System Modeling and Analysis*. New York, NY: CRC Press, 2001.

[23] S. Boyd, "CVX: Matlab software for disciplined convex programming," Mar. 2014. [Online]. Available: http://cvxr.com/cvx/

[24] IEEE Power and Energy Society. (2010, Sep.) Distribution test feeders. [Online]. Available: http://www.ewh.ieee.org/soc/pes/dsacom/testfeeders/index.html

[25] "Commercial and residential hourly load profiles for all TMY3 locations in the United States," Jul. 2013. [Online]. Available: http://en.openei.org/doe-opendata/dataset/